Quasielastic neutron scattering study of diffusive hydrogen motion in $ZrBe_2H_{0.56}$

R. L. Cappelletti, Z. Chowdhuri, T. J. Udovic, and R. M. Dimeo
NIST Center for Neutron Research, National Institute of Standards and Technology, Gaithersburg, Maryland 20899-8562, USA

B. C. Hauback and A. J. Maeland
Institute for Energy Technology, P.O. Box 40, Kjeller, NO-2027 Norway

(Received 22 March 2006; revised manuscript received 12 May 2006; published 19 June 2006)

In $ZrBe_2H_{0.56}$ above 500 K, Be planes are separated by hexagonal Zr planes in the AlB_2 structure with the *H* atoms occupying interstitial sites that form a honeycomb net in the Zr planes. The data from quasielastic neutron scattering using two spectrometers covering a wide range of resolutions from 1 μeV to 64 μeV can be fitted with a simple model using only two parameters for all momentum transfers at each temperature. The parameters are an elasticlike fraction and the hopping rate associated with a quasielastic contribution described by two-dimensional nearest-neighbor uncorrelated hopping among the partially occupied interstitial sites. The temperature dependence of the hopping rate follows an Arrhenius relation with an activation enthalpy of (0.30±0.02) eV.

DOI: 10.1103/PhysRevB.73.224109 PACS number(s): 78.70.Nx

I. INTRODUCTION

Intermetallic $ZrBe_2$ crystallizes in the hexagonal AlB_2 structure with alternating planes of Zr and Be atoms. Zr occupies (0,0,0) in the unit cell. The Be atoms occupy (1/3,2/3,1/2) and (2/3,2/3,1/2) positions that lie on a honeycomb net. The structure of the hydrides $ZrBe_2H_x$ depends on the *H* concentration, *x*, and temperature. $ZrBe_2H_x$ is of interest since *H* diffuses rapidly and also because the diffusion is apparently two dimensional (2D), i.e., largely confined to the interstitial sites of the Zr planes that also form a honeycomb net. In this paper we describe an incoherent quasielastic neutron scattering study of the unusual diffusive motion of *H* in this system. While the system can host up to $x=1.5$, here we focus on a temperature regime (above 500 K) and hydrogen concentration ($x=0.56$) in which the sample is structurally in a single phase, that of $ZrBe_2$. Moreover, the *H* content is low enough to meet two other conditions, namely, to have a sample thin enough to be able to neglect multiple scattering corrections in the analysis of the neutron scattering results, and, as will be discussed, to be in a regime where correlated motion has little effect on the line shape, so that a dilute-regime model may be applied.

II. EXPERIMENTAL PROCEDURES

The $ZrBe_2$ sample was prepared by arc melting, followed by pulverization and hydriding at room temperature and atmospheric pressure to $ZrBe_2H_{1.5}$ (for details, see Ref. 1). Subsequent controlled hydrogen removal by evacuation at 673 K reduced the *H* content to 0.56±0.04. This value was corroborated by neutron prompt gamma activation analysis at the National Institute of Standards and Technology (NIST) (Ref. 2). A neutron diffraction powder pattern at 500 K is shown in Fig. 1. It was analyzed using the EXPGUI (Ref. 3) package implementing GSAS (Ref. 4). Apart from small peaks representing the minority Be_5Zr phase ($\approx$1% of the intensity), the pattern is reasonably well accounted for by a single hexagonal structure of the AlB_2 type, space group *P*6/*mmm*, with zirconium at (0,0,0), beryllium at (1/3,2/3,1/2), and hydrogen occupying the interstitial positions at (1/3,2/3,0). The results of the refinement give $a=3.8140$ Å and $c=3.2755$ Å for the dominant phase.

The 2.3 g sample was placed in an aluminum foil wrapper inserted into the 0.27 mm thick annulus of an aluminum sample can sealed under He. The can was mounted on a closed-cycle He refrigerator for measurements on the high flux backscattering spectrometer (HFBS). The annular dimension was chosen to give 90% neutron transmission in order to reduce the multiple scattering contribution to the total scattering within the sample. The dynamical range chosen for this experiment, ±36 μeV, gives an elastic peak resolution of 1.0 μeV full width at half maximum (FWHM). In order to reduce the data to extract the sample spectra, measurements were also made with an empty sample can

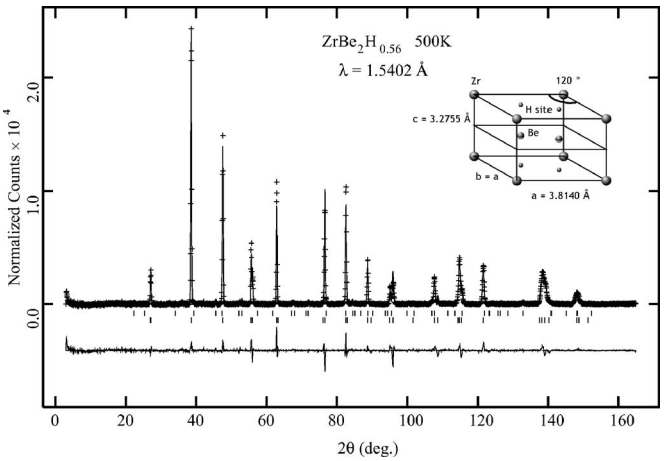

FIG. 1. Neutron diffraction pattern of $ZrBe_2H_{0.56}$. The solid line through the data represents the fit, the tick marks below the pattern represent the angular positions of the minority phase peaks (upper) and majority phase peaks (lower). The solid line below the pattern represents the difference curve. The background has been subtracted. Inset: small balls indicate *H* sites in the unit cell of the majority phase.

(6 h). A 9 h run on the sample at 50 K was made to establish a resolution function for each detector group. Runs lasting 10 h were then made at increasing temperaratures of 530, 560, and 580 K, and then at 570 K.

The same sample and can arrangement measured with the HFBS was used for measurements on the disk chopper spectrometer (DCS). Data reduction required measurements of an empty sample can, a vanadium rod for detector normalization, and the fast neutron background. The majority of DCS measurements were made with an incident wavelength of 6 Å resulting in an elastic peak resolution of 63.9 μeV FWHM. Seven 9 h runs were made at various temperatures: 300 K (for instrumental resolution), 520, 530, 540, 550, 560, and 580 K. In addition, the DCS settings were changed to give an incident wavelength of 7 Å with a resolution at the elastic peak of 20.3 μeV FWHM for 2 h runs at 300 K (for instrumental resolution) and 580 K.

III. THEORY

The best fit to the diffraction pattern in Fig. 1 is a structure in which the hydrogen is confined to the Zr planes. This confinement makes three-dimensional (3D) diffusion of H unlikely, since the H atoms would have to pass through inhospitable Be planes to arrive at acceptable sites in next nearest neighbor Zr planes that are a distance of 3.2745 Å away. Compare this to a nearest-neighbor-site in-plane distance of 2.2020 Å (see below). Moreover, nuclear magnetic resonance (NMR) measurements on a sample of $ZrBe_2H_{1.4}$ have their most convincing interpretation in terms of 2D diffusion.[5,6] (This is not to say that hopping in the third dimension is forbidden, but simply that it is unlikely to dominate the dynamics measured here.) These results suggest that the observed quasielastic scattering might be accounted for simply by an extension to the non-Bravais honeycomb net of the Chudley-Elliot[7] model of uncorrelated nearest-neighbor (NN) hopping among the partially occupied interstitial sites. Correlation has been found to have little effect on the *line shape* at this concentration, as discussed below. The hopping distance between NN sites is $d=a/\sqrt{3}$, where a is the lattice parameter in the plane. At 500 K, $d=2.2020$ Å. This value is used in subsequent data-fitting, ignoring changes with temperature, which are thought to be less than 1%.

Following the development in Rowe *et al.*[8] modified for the two-dimensional honeycomb net,

$$\frac{d^2\sigma_{inc}}{d\Omega d\omega} = \frac{\sigma_{inc}}{4\pi}\frac{k}{k_0}N_H e^{-pQ^2}F_{inc}(\mathbf{Q},\omega), \tag{1}$$

where $\sigma_{inc}=4\pi b_{inc}^2$ is the incoherent scattering cross section, b_{inc} is the H incoherent scattering length, $k(k_0)$ is the scattered (incident) neutron wave vector, N_H is the number of H nuclei, $\hbar\omega$ is the energy transferred by the neutron, e^{-pQ^2} is the vibratory Debye-Waller factor, and

$$F_{inc}(\mathbf{Q},\omega) = \frac{1}{2\pi}\left[\frac{(1+\cos\phi)(r-|A|)}{\omega^2+(r-|A|)^2} + \frac{(1-\cos\phi)(r+|A|)}{\omega^2+(r+|A|)^2}\right], \tag{2}$$

where

$$A = r[e^{i\mathbf{Q}\cdot\mathbf{d}_1} + e^{i\mathbf{Q}\cdot\mathbf{d}_2} + e^{i\mathbf{Q}\cdot\mathbf{d}_3}]/3 = |A|e^{i\phi}. \tag{3}$$

In the above equation, r is the hopping rate ($r=1/\tau$, where τ is the mean residence time: the model envisions H sitting and vibrating at interstitial sites for a time τ between jumps), and $\{\mathbf{d}_j\}$ are the vectors connecting an interstitial site to its three symmetrically-arrayed, equally-spaced NN sites in the plane. (There are two inequivalent sets of these vectors for this non-Bravais net, the one being simply the negative of the other.) For lowest order in Q, Eq. (2) reduces to

$$F_{inc}(\mathbf{Q},\omega) = \frac{1}{2\pi}\left[\frac{DQ^2\sin^2\theta}{\omega^2+(DQ^2)^2\sin^4\theta}\right], \tag{4}$$

where θ is the angle between the normal to the plane and $\mathbf{Q}$, and

$$D = \frac{d^2}{4\tau} \tag{5}$$

is the self-diffusion coefficient. The expression of Eq. (4) does not depend any longer on the geometry of the lattice except for its dimensionality. As expected, the expression for D in Eq. (5) is the same as that for a random walk in two dimensions in steps of length d.

The expression in Eq. (2) was averaged for this powder sample equally over all directions of $\mathbf{Q}$ and convolved with the resolution function for each group of detectors of the appropriate spectrometer to compare with measured spectra. Besides quasielastic scattering, all measured spectra were found to contain an elasticlike scattering contribution. The model above has an elastic contribution precisely for $\mathbf{Q}$ perpendicular to the H-containing planes, as can be seen from Eq. (2). When Eq. (2) is averaged uniformly over $\mathbf{Q}$ directions for our powder sample and convolved with the resolution function, this elastic contribution was found to be insufficient to account for the observed elasticlike scattering.

In order to obtain good fits of the model to the measured spectra, an additional term was necessary that we shall call an elasticlike term. Before convolving with the resolution function, the model is described by a scattering cross section that is proportional to:

$$f\delta(\omega) + (1-f)F_{inc}(\mathbf{Q},\omega), \tag{6}$$

where f is the elasticlike fraction, i.e., the elasticlike contribution not included in F_{inc}. In analyzing the spectra, care was taken to exclude detectors for Q values in the vicinity of Bragg peaks, so that the observed elasticlike scattering could only arise from diffuse coherent scattering, expected to be small and Q dependent, or incoherent scattering from relatively immobile H. In fact, f has been found to be both independent of Q and between 13 and 14.5% for backscattering data, depending on temperature, which suggests that it arises from an H component having much lower mobility than the diffusing component. The form of Eq. (6), in which elasticlike and inelastic components are assumed to have equal scattering lengths, is consistent with the elasticlike component arising predominantly from H.

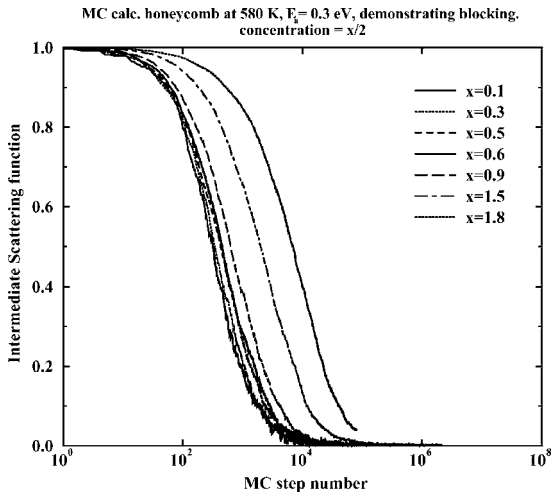

FIG. 2. Powder-averaged incoherent intermediate scattering function at $Q=1.51$ Å and 580 K with an activation energy of 0.3 eV calculated using a Monte Carlo technique for the honeycomb net at various occupation levels to test the importance of correlation effects on line shape. Note that for x values below $x=0.9$ there is little change.

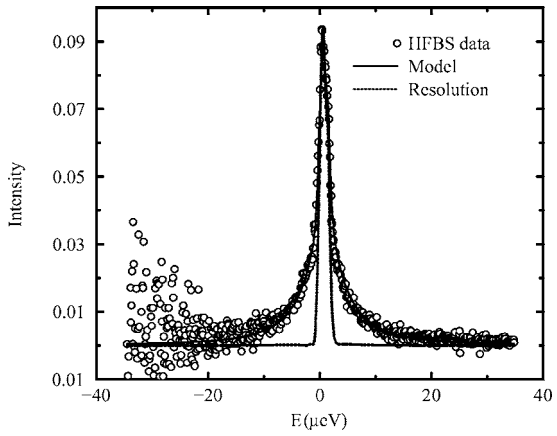

FIG. 3. HFBS spectrum at 580 K at an incoming neutron wavelength of 6.27 Å over the dynamic range from -36 μeV to 36 μeV at $Q=0.37$ Å^{-1}. The resolution curve shown (dotted line) is taken from fitting a sum of Lorentzians to the spectrum at 50 K. The fitted results to the model described in Sec. III for parameters $r=35.69$ μeV and $f=0.1293$ are shown as a solid line.

An alternative attempt to describe the scattering without including an elasticlike term is a two-state model that includes trapping. Following the development in Hempelmann's text,[9] the two-state model treats the diffusing atoms as being either "free" or "trapped." The atoms diffuse freely, as described by the NN uncorrelated hopping model detailed above, until they are trapped at a rate r_1. While trapped, they remain fixed on average until they escape at a rate r_0. The resulting rather complicated expression for the scattering function, an elaboration of Hempelmann's Eq. (5.172) for our case, does not reduce simply to a sum of Lorentzians, making it necessary to convolve numerically with the resolution function after powder averaging, and therefore making the fitting procedure over the parameter space of r, r_0, and r_1, prohibitively time consuming. Therefore, a less thorough investigation procedure "by hand" was employed over more than a hundred judiciously chosen parameter sets. None of the resulting comparisons with data were deemed satisfactory. We conclude from this attempt that the elasticlike peak is likely due to trapping at defects having a *distribution* of trapping energies.

Incoherent scattering measures the time self-correlation function of each particle, summed over all particles. Nonetheless, any given particle may be temporarily hindered in its diffusive motion by the presence of blocking particles on neighboring sites, and in this sense the measurement is sensitive to correlations in the motion of the one particle with all the others. In the model above we have ignored such correlations, i.e., the model represents the dilute limit in which each particle diffuses among the allowed sites as if no other particles were present. In this section we examine in what sense this approximation is suitable at the present concentration.

We employ a Monte Carlo (MC) method to do this. The system is represented by a 100×100 honeycomb decorated by N particles initially located on the lattice sites with a probability taken from a pseudorandom distribution. A poll is conducted by randomly selecting a particle and randomly selecting one of its NN sites. If the site is occupied, no jump is made, and the poll proceeds to again select a particle randomly. If the site is not occupied, a jump is allowed according to a probability selected from a distribution associated with the input temperature and activation energy. The displacement of each particle is traced in this way, continuing the trajectory, if necessary, across a boundary by repeating the lattice periodically. N executions of the poll constitute one MC step. Computations up to 2^{21} MC steps were made.

The parameters of interest in this calculation may be introduced by writing the expression for the self-diffusion constant in the presence of correlations.

$$D=\frac{d^2(1-c)f_t}{4\tau'}, \tag{7}$$

where $1-c$ is the blocking factor, f_t is the self-diffusion correlation factor, and τ' is the mean residence time in the absence of correlation effects. The blocking factor accounts for jump prevention by the statistical occupation of a NN site, and the correlation factor for "memory" effects contributing to the hindering of the motion. At a concentration of $x=1.5$ corresponding to a 3/4 filled net ($c=0.75$), the correlation factor was determined to be $f_t=0.40$ from the infinite temperature long-time slope (approximately the last third of 2^{17} MC steps) of the average mean-square displacement (MSD) as a function of a MC step number. This value is in reasonable agreement with a previous MC calculation for the honeycomb net by Kutner[10] who obtained $f_t=0.45$ at this filling value.

To test the effects of correlations on the measured line shapes, we have used the MC method to calculate the powder-averaged intermediate scattering function (ISF) as a function of the MC step number. A plot of the ISF for various concentrations is shown in Fig. 2 where it is seen that the effect of correlations on the *shape* of the line becomes pro-

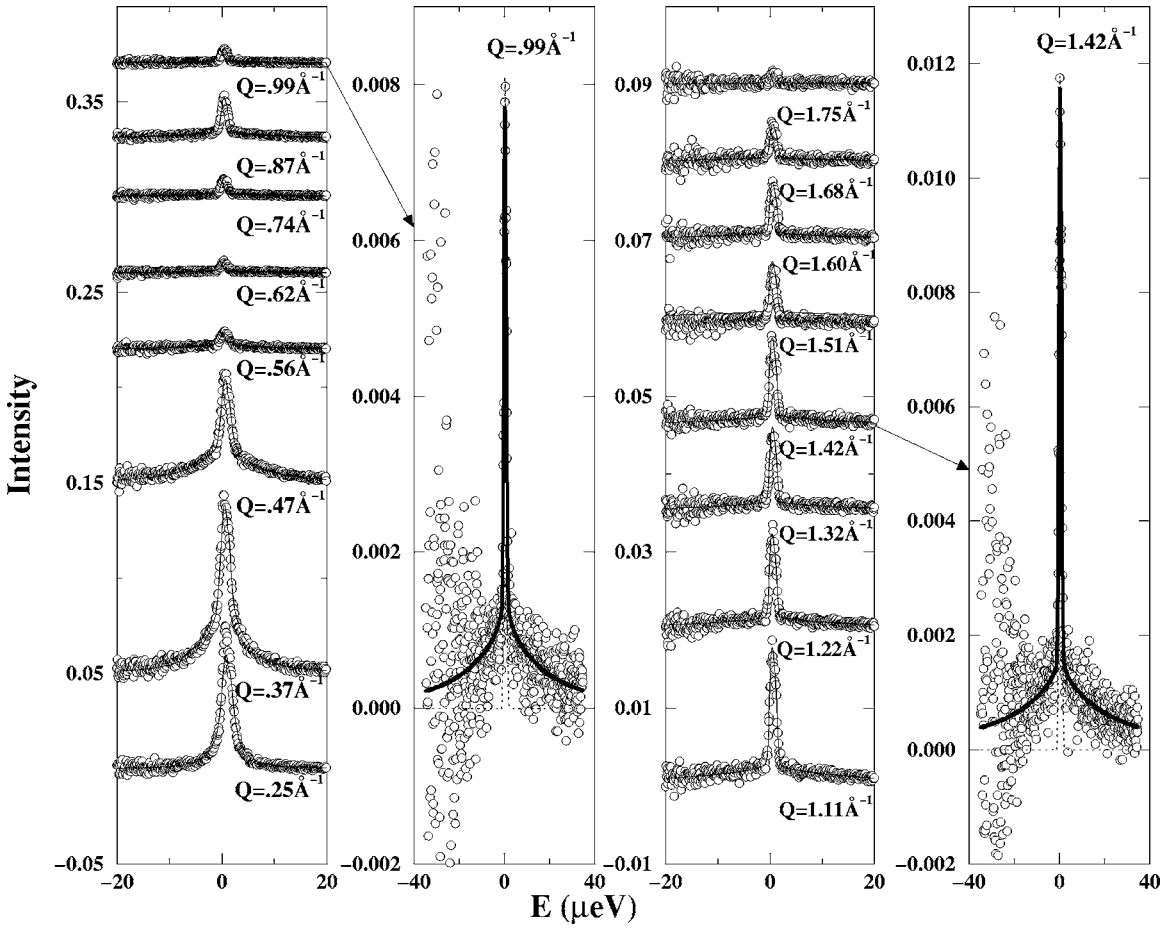

FIG. 4. HFBS spectra at 580 K at an incoming neutron wavelength of 6.27 Å over the dynamic range from −36 μeV to 36 μeV for all detector groups with Q values as indicated. From left to right, panels 1 and 3 show the spectra over a reduced range; panels 2 and 4 show the spectra over the full range for selected Q values. The dotted curves in panels 2 and 4 are resolution curves while the solid curves are the results of fits to the model for parameters $r=35.69$ μeV and $f=0.1293$.

nounced beyond $x=0.9$. As discussed above, some of the H atoms are relatively immobile, so at the present concentration, $x=0.56$, we may safely employ the dilute limit Chudley-Elliott model in making fits. Since correlations are present in the actual system, the values of τ taken from fitting the dilute model to the data must already include the effects of both the blocking and correlation factors. Neither of these factors is dependent on temperature, thus any systematic errors introduced by using a dilute-limit model to fit the data should not propagate into the temperature dependence of τ.

IV. DATA TREATMENT AND EXPERIMENTAL RESULTS

The reduced data were fitted to the model described above using a specially adapted program within the data analysis and visualization environment (DAVE) data treatment suite available at the NIST Center for Neutron Research (NCNR).[11] This program is able to simultaneously fit the several spectra at a given temperature corresponding to detector groups at available Q values by adjusting the two model parameters r and f. For each group, the model is convolved with the measured resolution function. A feature of the program that saves time is that the convolution is carried out analytically by first fitting the resolution functions with sums of Lorentzians. Since the model in Eq. (2) involves only Lorentzians, the convolution may be written as a sum of Lorentzians before numerically powder averaging.

An example spectrum taken from 580 K HFBS data ($\approx$1 μeV resolution) along with the fit result is shown in Fig. 3. The data for all the HFBS spectra at 580 K are shown in Fig. 4. Little correlation is found between the adjustable parameters r and f in fitting these HFBS data, and hence we regard the obtained values as being reliable. Plots of HFBS data at all measured temperatures (not displayed here) resemble those in Fig. 4 in terms of the quality of the fits.

The same program was used to treat DCS data after first restricting the spectrum to ±1.3 meV for the 6 Å data and to ±0.7 meV for the 7 Å data. In fitting the DCS data, a strong correlation was found between the fitting parameters r and f, rendering their independent determination unreliable. For this reason, parameters were taken from the backscattering results and curves generated for comparison to the DCS measurements. Data at 6 Å and 580 K are shown in Fig. 5, where it is seen that, while the behavior in the wings is reasonably well accounted for, the elasticlike peak is not. This is particularly evident in the higher Q data. The impli-

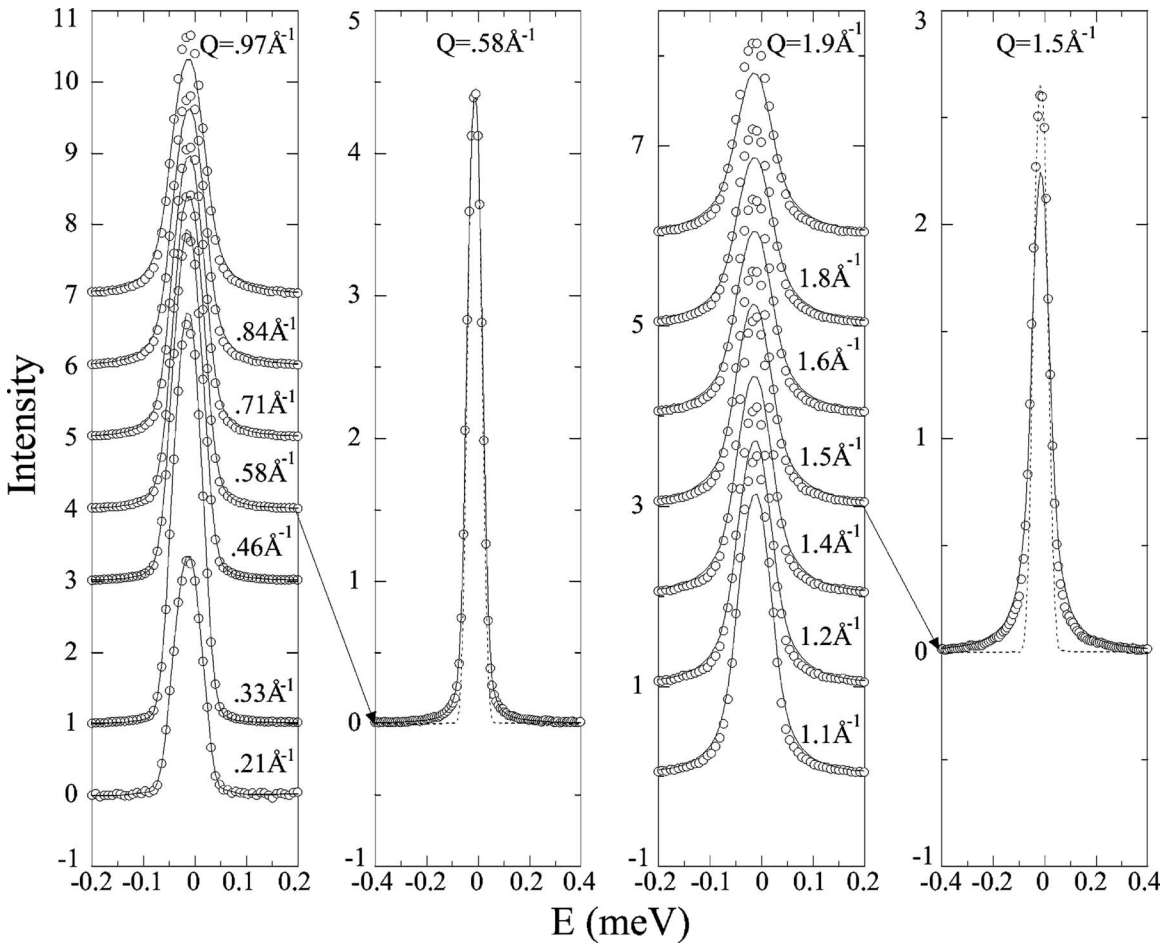

FIG. 5. DCS spectra at 580 K over the dynamic range from −0.4 meV to 0.4 meV for all detector groups at an incoming neutron wavelength of 6 Å. From left to right, panels 1 and 3 show the spectra over a reduced range; panels 2 and 4 show spectra over a broader range for selected Q values. The dotted curves in panels 2 and 4 are resolution curves. The solid curves are the results of a model calculation using parameters taken from the fit to HFBS data shown in Fig. 4, $r=0.035\,69$ meV and $f=0.1293$, illustrating a lack of agreement in the elasticlike region. Compare resolutions (64/1) to the HFBS data in Fig. 4.

cation is that the r parameter, which tends to govern behavior in the wings, is correctly accounting for these data on the much larger energy scale ($\approx 64\ \mu$eV resolution) of DCS compared to HFBS.

Since the fit in the wings is determined mainly by r, an alternative procedure is to take the r parameter from HFBS data and to fit the DCS data by letting only f vary. An example at 580 K for one detector group is shown in Fig. 6 and for all the spectra at that temperature in Fig. 7. This procedure clearly results in a better fit. The f value is larger than that obtained from fitting backscattering data that are 64 times higher in resolution.

The data at 7 Å incident wavelength ($\approx 20\ \mu$eV resolution) have been fitted in a similar manner. As at 6 Å, one finds that the adjustable parameters are strongly correlated in fitting the 580 K data. Hence, we used the r and f values from the HFBS during the fitting and display the results in Fig. 8. As in the 6 Å data, the wings are reasonably well acccounted for, but the elasticlike peak is not. Again, the r value was fixed at the HFBS value and f allowed to vary during the fitting. The results are displayed in Fig. 9. The fit is much better, and the f parameter is between that of the fit to the 6 Å data and to backscattering data.

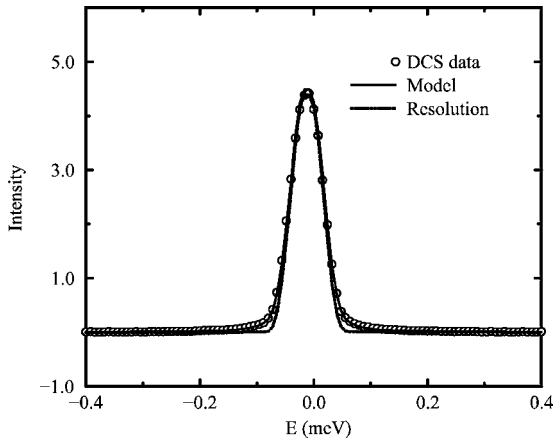

FIG. 6. DCS spectrum at 580 K over the dynamic range from −0.4 meV to 0.4 meV at $Q=0.56$ Å^{-1} at an incoming neutron wavelength of 6 Å. The resolution curve shown (dotted line) is taken from fitting a sum of Lorentzians to the spectrum at 300 K. The fitted results to the model described in Sec. III for parameters $r=0.035\,69$ meV and $f=0.3325$ are shown as a solid line.

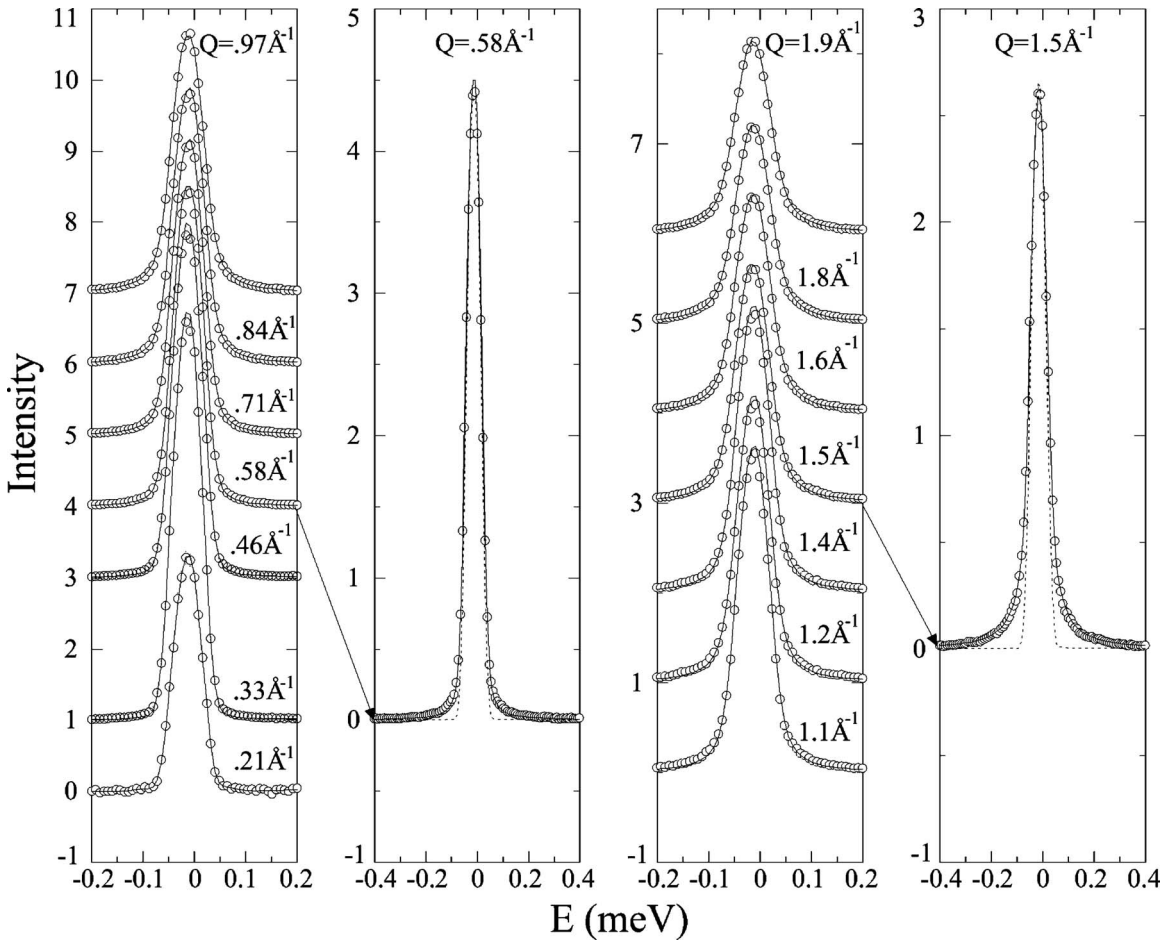

FIG. 7. DCS spectra at 580 K over the dynamic range from −0.4 meV to 0.4 meV for all detector groups at an incoming neutron wavelength of 6 Å. From left to right, panels 1 and 3 show the spectra over a reduced range; panels 2 and 4 show spectra over a broader range for selected Q values. The dotted curves in panels 2 and 4 are resolution curves. The solid curves are the results of a model calculation using the fitting parameter $r=0.035\,69$ meV taken from the fit to HFBS data shown in Fig. 4 and varying f, resulting in $f=0.3325$. There is now good overall agreement compared to Fig. 5. At this resolution (64 μeV) the value of f is larger than from the fit to HFBS data. Compare resolutions (64/1) to the HFBS data in Fig. 4.

V. DISCUSSION

The fact that the quasielastic portions of the spectra for all Q values at resolutions ranging from $\approx 1\ \mu$eV to $\approx 64\ \mu$eV are well described by the same hopping parameter at a given temperature lends credibility to the basic correctness of applying the Chudley-Elliott model, specialized to NN 2D hopping on the honeycomb net, to this $ZrBe_2H_{0.56}$ system. As discussed above, detailed Monte Carlo calculations that reproduce the results of previous Monte Carlo studies[10] which display hopping correlations at higher concentrations show that they have little effect on the line shape at this concentration. NMR work has made a significant contribution to establishing the 2D nature of the diffusion in this hydride family.[5,6,12,13] The values of the activation enthalpy obtained by NMR measurements on samples of $ZrBe_2H_{1.4}$ are $(0.27\pm0.02$ eV)[5] and $(0.25\pm0.02$ eV)).[6] Figure 10 is an Arrhenius plot of r vs 1000/T which yields a value of the activation enthalpy of 0.30 ± 0.02 eV, where the uncertainty is an estimate including both random and systematic errors, in good agreement with the NMR results. Values of r taken from fitting HFBS data were used in this plot. The NMR values arise from data taken over a considerably wider temperature range than in the present work. Our range was limited at the lower end to be well above a transition to an ordered phase at ≈ 485 K,[14] and at the upper end by our apparatus. The agreement between the activation enthalpies determined from neutron and NMR measurements suggests that hydrogen concentration plays only a small role in modifying the average potential energy landscape experienced by the H ions as they diffuse about.

The prefactor r_0 in the Arrhenius expression corresponds to a residence time $\tau_0=(2.8\pm0.5)\times10^{-13}$ s. We can use this value and Eq. (5) to calculate a prefactor in the corresponding Arrhenius expression for the self-diffusion coefficient, $D_0=4.3\times10^{-8}$ m^2 s^{-1}, at $x=0.56$. A comparison of this result to results at concentration c requires multiplying by the product $(1-c)f_t$ introduced in Eq. (7) for that c, and dividing by the product for $x=0.56$, (i.e., for $c=0.28$), namely

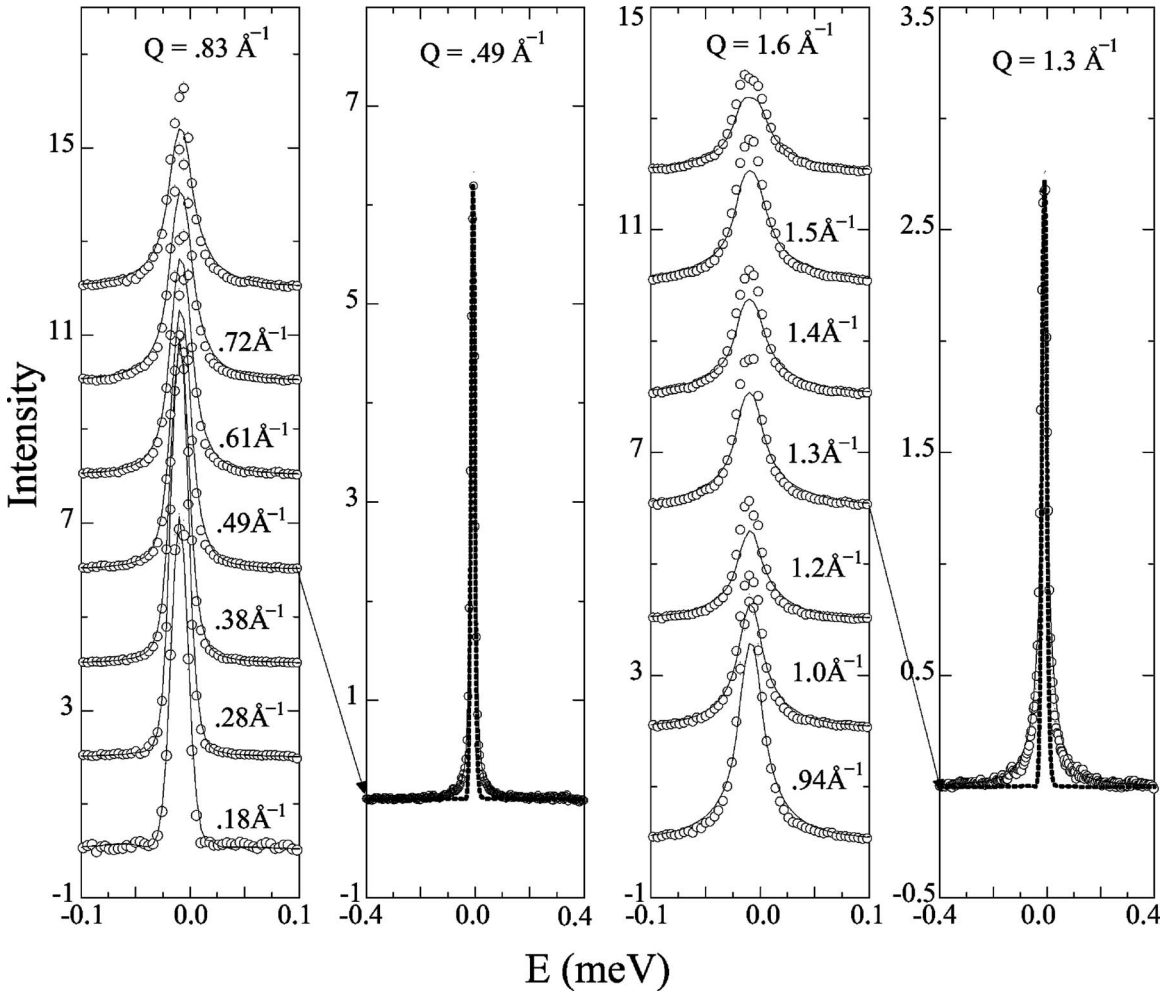

FIG. 8. DCS spectra at 580 K over the dynamic range from −0.4 meV to 0.4 meV for all detector groups at an incoming neutron wavelength of 7 Å. From left to right, panels 1 and 3 show the spectra over a reduced range; panels 2 and 4 show spectra over a broader range for selected Q values. The dotted curves in panels 2 and 4 are resolution curves. The solid curves are the results of a model calculation using parameters taken from the fit to HFBS data shown in Fig. 4, $r=0.035\,69$ meV and $f=0.1293$, illustrating a lack of agreement in the elasticlike region. Compare resolutions (20/1) to the HFBS data in Fig. 4 and (20/64) to the 6 Å DCS data in Fig. 5.

(0.72×0.75), where the second term was obtained from our MC calculation.

The presence of an extra elasticlike term is not unusual in itself, nor is its interpretation in terms of a component of relatively immobile (e.g., trapped) H atoms.[15] H may be trapped in various kinds of defect sites that surely exist in this powder sample (point defects, grain boundaries, strained regions, etc.). There is a distribution of trapping energies associated with the various kinds of defects. The more deeply bound particles will lead to less broadening of the line. At a lower resolution, the elasticlike fraction is larger than at higher resolution since even the lightly bound particles appear under the elastic peak. Thus a variation of f by a factor of 2.5 while the resolution varies by a factor of 64 may not be unreasonable. Trapping in a variety of environments offers a way, in principle, to understand the larger values of f obtained from fitting DCS data compared to those from fitting HFBS data. Detailed estimates would depend on knowledge of defect and trapping energy distributions in this sample, which is not currently nor likely to be available.

Nonetheless, some insight may be gained from a simple model that assumes one type of trapping (Tr) site with a binding energy E_b (compared to free sites) that constitutes a fraction N_{Tr}/N_s of all the sites, N_s. The thermal occupation of these sites, $\langle n_{Tr}\rangle$, is governed by a population exchange with the "free" particles according to the equation

$$\langle n_{Tr}\rangle = \frac{\sum_{n_{Tr}}^{N_{Tr}}\sum_{n_F}^{N_F} n_{Tr} z^{n_{Tr}} \binom{N_{Tr}}{n_{Tr}}\binom{N_F}{n_F}}{\sum_{n_{Tr}}^{N_{Tr}}\sum_{n_F}^{N_F} z^{n_{Tr}} \binom{N_{Tr}}{n_{Tr}}\binom{N_F}{n_F}}, \tag{8}$$

where $z=\exp\left(\frac{E_b}{k_BT}\right)$, N_F is the number of free sites, and n_F is the number of particles occupying them. $n_F+n_{Tr}=N$, the number of particles in the lattice, which introduces a condition restricting the sums. (Having more than one type of trap complicates the formula and puts more constraints on the sums.) Examples of occupation curves versus temperature

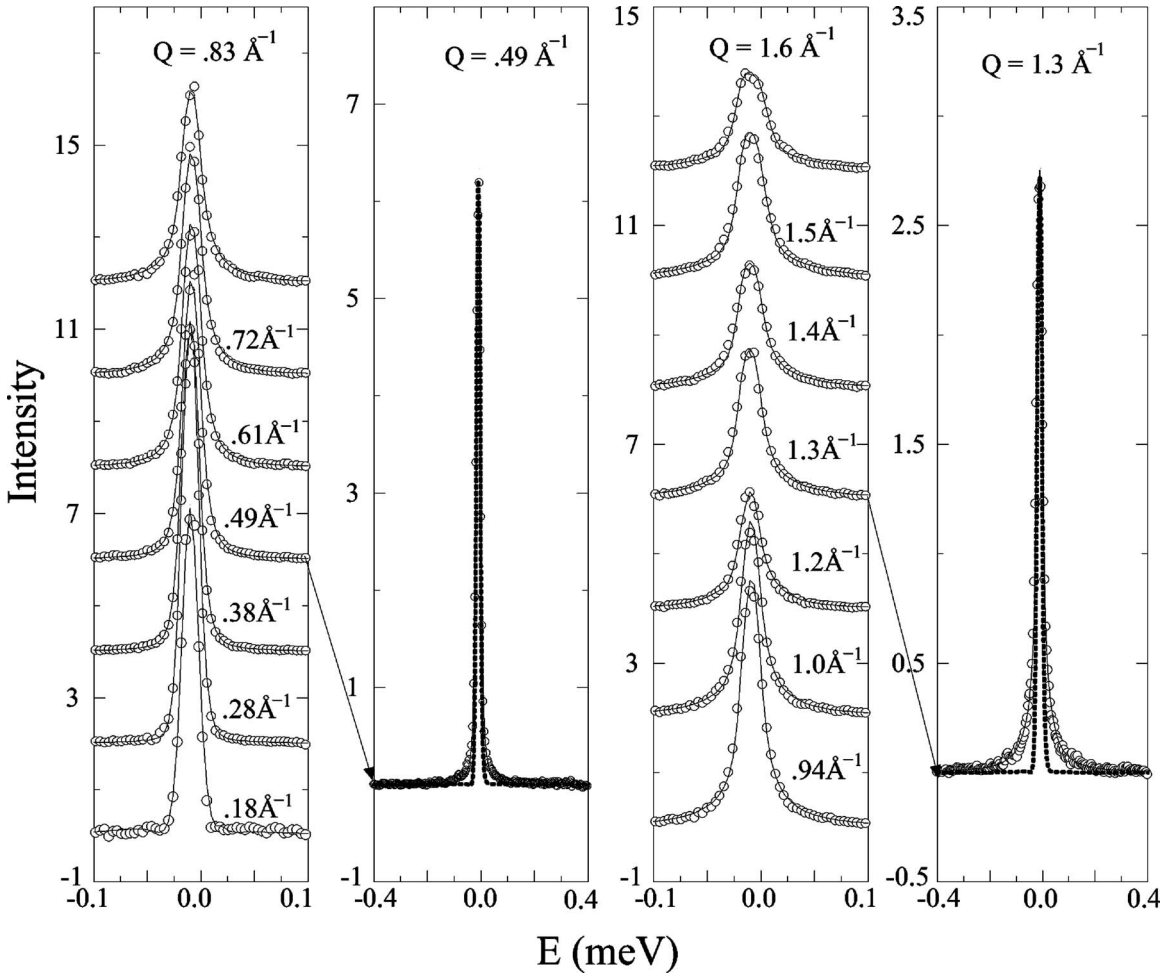

FIG. 9. DCS spectra at 580 K over the dynamic range from −0.4 meV to 0.4 meV for all detector groups at an incoming neutron wavelength of 7 Å. From left to right, panels 1 and 3 show the spectra over a reduced range; panels 2 and 4 show spectra over a broader range for selected Q values. The dotted curves in panels 2 and 4 are resolution curves. The solid curves are the results of a model calculation using the fitting parameter $r=0.035\,69$ meV taken from the fit to HFBS data shown in Fig. 4 and varying f, resulting in $f=0.3120$. There is now good overall agreement compared to Fig. 8. At this resolution (20 μ eV) the value of f is larger than the HFBS result, but less than the 6 Å DCS result. Compare resolutions (20/1) to the HFBS data in Fig. 4 and (20/64) to the 6 Å DCS data in Fig. 7.

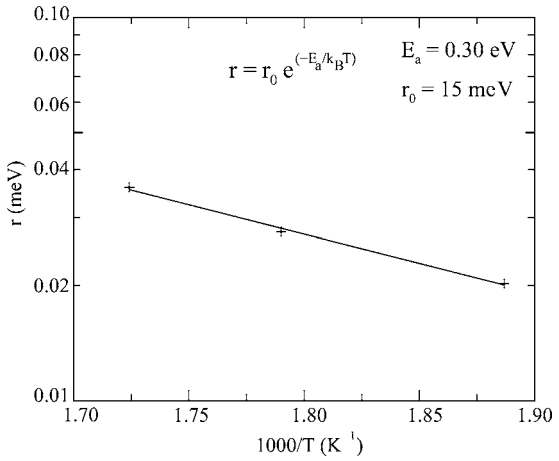

FIG. 10. Activation enthalpy, E_a, and prefactor, r_0, from an Arrhenius plot of the hopping rate r taken from fits to HFBS data.

for one and two trap types are shown compared to the HFBS results in Fig. 11. There we see qualitatively that even a few percent of trap sites can lead to a significant fraction of *particles* being trapped. It is also apparent that a distribution of even more than two trap types is needed to account for the HFBS results.

In addition to the two-state model described in Sec. III B, other models were tried in search of alternative explanations for the observed elasticlike scattering contributions, but the fits were not convincing. One model investigated supposed no extra elasticlike term, but that each diffusing particle could jump around at some rate in a confined region (e.g., between two neighboring sites) before moving on. There are two adjustable parameters in this model: r_1 for the confined motion and r_2 for the motion over all the sites. Such confinement gives rise to a Q-dependent elastic incoherent structure factor contribution to the quasielastic scattering, contrary to what is observed experimentally.

We more directly investigated the possibility that the elasticlike contribution arises from correlated motion using the

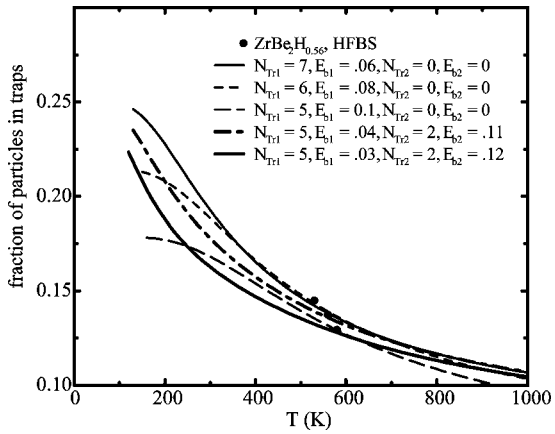

FIG. 11. The dots represent the elasticlike fraction f from fits to HFBS data. The curves are calculated for the various parameters indicated (with binding energies in eV), from Eq. (8) for one type of trap and a from a similar formula for two types. In each case there are 100 sites and 28 particles.

MC method. An MC-generated ISF was converted by Fourier transformation to a scattering function of pseudoenergy that differs from true energy by an adjustable conversion factor relating a real time interval to MC stepsize. Trying a series of conversion factors, this line shape was convolved with the appropriate resolution function to compare with HFBS results. For conversion factors that sufficiently broadened the line shape to match the wings qualitatively, there always remained a significant deficiency in the elasticlike region, as with the dilute model.

VI. CONCLUSION

The present neutron quasielastic scattering measurements on a single-phase $ZrBe_2H_{0.56}$ sample having the AlB_2 structure made on two spectrometers with widely different resolutions can be successfully interpreted in terms of a simple two parameter model at each temperature for all momentum transfers measured. This model incorporates two-dimensional NN uncorrelated activated H hopping along with an extra elasticlike term to account for a relatively immobile H fraction. Similar to NMR in which a single residence time τ is able to account for all the data at a given temperature,[5,6] a single τ accounts for the quasielastic data at all resolutions for all Q values measured at a given temperature. The self-diffusion coefficient has been determined for temperatures between 530 and 580 K. The activation enthalpy is inferred to be (0.30 ± 0.02) eV, in agreement with the NMR result for $ZrBe_2H_{1.4}$.

ACKNOWLEDGMENT

This work utilized facilities supported in part by the National Science Foundation under Agreement No. DMR-0454672.

[1] A. F. Andresen, K. Otnes, and A. J. Maeland, J. Less-Common Met. **89**, 201 (1983).
[2] Prompt gamma measurements courtesy of R. Paul of the NIST Analytical Chemistry Division, Nuclear Methods Group.
[3] B. H. Toby, J. Appl. Crystallogr. **34**, 210 (2001).
[4] A. C. Larson and R. B. Von Dreele, Los Alamos National Laboratory Report LAUR 86-748 (2000).
[5] A. F. McDowell, C. F. Mendelsohn, Mark S. Conradi, R. C. Bowman, Jr., and A. J. Maeland, Phys. Rev. B **51**, 6336 (1995).
[6] F. Kimmerle, G. Majer, U. Kaess, A. J. Maeland, M. S. Conradi, and A. F. McDowell, J. Alloys Compd. **264**, 63 (1998).
[7] C. T. Chudley and R. J. Elliott, Proc. Phys. Soc. London **77**, 353 (1961).
[8] J. M. Rowe, K. Sköld, H. E. Flotow, and J. J. Rush, J. Chem. Phys. **32**, 41 (1971).
[9] Rolf Hempelmann, *Quasielastic Neutron Scattering and Solid State Diffusion* (Oxford University Press, NY, 2000), p. 131.
[10] Ryszard Kutner, J. Phys. C **18**, 6323 (1985).
[11] http://www.ncnr.nist.gov/dave
[12] V. Kodibagkar, J. L. Herberg, R. C. Bowman, Jr., and M. S. Conradi, J. Alloys Compd. **330–332**, 179 (2002).
[13] A. F. McDowell, P. A. Fedders, and M. S. Conradi, Phys. Rev. B **58**, 248 (1998).
[14] T. J. Udovic, Q. Z. Huang, and R. L. Cappelletti (unpublished).
[15] D. Richter, R. Hempelmann, and R. C. Bowman, in *Hydrogen in Intermetallic Compounds II*, edited by L. Schlapbach, Topics in Applied Physics (Springer-Verlag, Berlin 1992), Vol. 67, p. 97.